SUPPLEMENTARY MATERIAL

Geodynamic history and mantle evolution recorded in Cenozoic lavas of Sardinia

G. Gisbert*[a]; Y. Cai[b]; D. Gimeno[c]

[a] Instituto de Geociencias (CSIC,UCM), Calle Dr. Severo Ochoa 7, 28040 Madrid (Spain). ggisbertp@hotmail.com
[b] Lamont-Doherty Earth Observatory, Columbia University, 61 Rt 9w, Palisades, NY 10964, (USA). cai@ldeo.columbia.edu
[c] Facultat de Geologia, Universitat de Barcelona, C/ Martí i Franquès s/n, 08028 Barcelona (Spain). domingo.gimeno@ub.edu

Sections:

1. PETROGRAPHY OF SULCIS VOLCANIC ROCKS

Petrographic observation of Sulcis volcanic rocks has revealed abundant textural variability within the volcanic sequence due to the presence of lava domes and flows and pyroclastic rocks, including the latter ignimbrite deposits with variable welding degrees.

Lava domes and flows are porphyritic (with the exception of Monte la Noce unit lava flows, which are aphyric), and consist of phenocrysts within a vitreous or partially crystallized groundmass which may present various degrees of devitrification. Enclaves may be present. Ignimbrite deposits consist of fragmentary material formed by pyroclasts, which include shards (fine vitreous fragments), pumice, crystals, and crystal fragments, and enclaves (either xenoliths or accidental lithics). Compacting and welding modified the original textures and structures of these deposits. They produced more cohesive rocks with eutaxitic texture evidenced by the elongation and flattening of shards and pumices. High welding degree and associated rheomorphism may conceal or even delete the original pyroclastic texture of an ignimbrite. Depending on their welding degree, ignimbrites appear differently affected by devitrification processes, which involve both the shards and pumices.

Regarding the mineral content there are mainly two different associations: the lower half of the volcanic succession (Andesites unit) and the rest of the sequence. Andesites present a mineral paragenesis which is dominated by plagioclase and pyroxenes. In the ignimbritic upper half of the sequence, the mineral paragenesis is dominated by feldspar (one or two), which is accompanied by opaque minerals (Fe and Ti oxides) and accessory mafic minerals. These mafic minerals are mainly pyroxenes, with presence in some units of amphibole or biotite. In comenditic units quartz may also be found. Zircon and apatite can be found as accessory minerals in some units. Vapour phase amphibole crystals, which may appear as poikilitic laths in the matrix (in comendites) or as hypidiomorphic crystals in vesicles (miarolitic texture in peralkaline or nearly peralkaline units), may be present.

Unit	Abbr.	Porphyricity	Mineral assemblage	Main characteristics
18/19	**CL/PG**	10	sa+pl+opq±zrn	**Colonne/Punta Genniò**: moderately welded cineritic ignimbrite
17	**PM**	<1	sa+ano+pl+opq+m.a.±zrn	**Punta Mingosa**: moderately welded aphyric cineritic ignimbrite
16	**SP**	1-20	pl+ano+opq+px+amp	**Serra di Paringianu**: extremely welded and eutaxitic ignimbrite. Abundant extremely flattened light and dark grey pumices. Basal vitrophyre. Non-welded facies in northern San Pietro and Santo Antioco islands
15	**PA**	<10	sa+pl+opq±bt±zrn	**Paringianu**: scarcely to moderately welded complex ignimbritic unit. Mostly cineritic. Low porphyricity and pumice content.
14	**CF**	10-20	sa+opq+ano	**Carloforte: Peralkaline**. Strongly welded and eutaxitic ignimbrite with abundant sanidine-bearing black pumices. Also grey and white pumices.
13	**MU**	<3	sa+qz+opq+zrn+amp(v)	**Monte Ulmus**: Peralkaline. Strongly welded and eutaxitic aphyric ignimbrite with occasional scarce black strongly flattened pumices. Basal vitrophyre.
12	**CO**	5-30 up to 50	sa+qz+amp+opq+amp(v)	**Comendites**: Peralkaline. Complex unit. Lava flows and variably welded ignimbrites with or without basal vitrophyre. May contain quartz phenocrysts
11	**MZ**	3-20	pl+bt+opq	**Matzaccara**: variably welded ignimbritic unit. Presents bronze-coloured biotite.
10	**MCR**	5-20	sa+pl+opq±zrn	**Montagna di Capo Rosso**: lava flows and moderately welded lithic rich ignimbrites.
9	**PC**	up to 50	ano+pl+opq+cpx+opx	**Punta dei Cannoni**: moderately to strongly welded, eutaxitic and porphyritic ignimbritic unit. Abundant big (several dm) pumices.
8	**NU**	20-30	sa+pl+opq+cpx±amp(v)	**Nuraxi**: extremely welded and eutaxitic ignimbrite. Scarce extremely flattened grey pumices. Rheomorphic structures are abundant. Basal vitrophyre.
7	**CA**	10	sa+pl+opq	**Conca is Angius**: slightly welded complex ignimbritic unit. Abundant pumices and accidental lithics. Degassing structures present.
6	**MC**	10-20	sa+pl+opq+amp(v)	**Monte Crobu**: moderately to extremely welded and eutaxitic ignimbrite. Abundant to dominant grey and occasionally black strongly flattened pumices. Rheomorphic. Basal vitrophyre.
5	**MLN**	<5	pl+opq±bt	**Monte la Noce**: lava flows, cinerites and moderately to extremely welded ignimbrites with basal vitrophyre. Aphyric.
4	**SE**	10-20	pl+opq+m.a.±opx±cpx +amp(v)	**Seruci**: highly welded and eutaxitic ignimbrite with dm-sized pumices. Basal vitrophyre.
3	**AC**	10-20	pl+bt+opq±amp	**Acqua sa Canna**: poorly welded ignimbrite, formed by several flows deposits with pumice normal grading. Locally lithic-rich.
2	**LE**	10-20	pl+sa+opq+opx±zrn	**Lenzu**: strongly welded and eutaxitic ignimbrite. Abundant dm-sized pumices. Basal vitrophyre.
1	**CM**	10-30	pl+cpx+opq±bt±amp	**Corona Maria**: scarcely to moderately welded and eutaxitic ignimbrite. Abundant pumices and lithic fragments. Basal vitrophyre.
AND	**AND**		pl+opx+cpx+opq±ol	**Andesites**: lava flows and domes with associated breccias

Main petrographic characteristics of the studied units. Abbr.; unit name abbreviation. Mineral abbreviations: amp: amphibole; ano: anorthoclase; bt: biotite; cpx: clinopyroxene; ol: olivine; opq: opaque mineral; opx: orthopyroxene; pl: plagioclase; px: pyroxene; qz: quartz; sa: sanidine; zrn: zircon; a.m.: altered mafic; (v): vapour phase.

2. SELECTION OF REPRESENTATIVE WHOLE ROCK GEOCHEMICAL DATA

In the following tables major, minor and trace element compositions and CIPW norm of representative samples from Sulcis Oligo-Miocene volcanism are presented. Rock classifications follow Le Maitre *et al.* (2002); FeO and Fe_2O_3 are calculated following Middlemost (1989). Mineral abbreviations: ab: albite; acm: acmite; an: anorthite; ap: apatite; crn: corundum; di: diopside; hyp: hyperthene; ilm: ilmenite; mag: magnetite; or: orthoclase; qz: quartz; rt: rutile; ttn: titanite. <LL: below the lower limit of the calibration range; these values are given as reference but not used in discussions. na: not analysed. Minor and trace element concentrations are in µg/g (ppm). 1: XRF data; 2: XRF data, ICP data when XRF data are below the calibration range; 3: ICP data, XRF data when ICP data are not available; 4: ICP data; *: ICP value of an element for which XRF data are used. Sampling location is provided in supplementary materials in Gisbert & Gimeno (2017).

References:

Gisbert, G., Gimeno, D., 2017: Ignimbrite correlation using whole-rock geochemistry: an example from the Sulcis (SW Sardinia, Italy). Geological Magazine 154, 740-756.

Le Maitre, R.W. (Ed.), 2002. Igneous Rocks: A Classification and Glossary of Terms. Recommendations of the International Union of Geological Sciences Subcommission on the Systematics of Igneous Rocks. Cambridge University Press, Cambridge.

Middlemost, E.A.K., 1989. Iron oxidation ratios, norms and the classification of volcanic rocks. Chemical Geology 77, 19-26.

Sample	VS-721	VS-786	VS-784	VS-782	VS-783	VS-763	VS-790	VS-788	VS-757	ISP-252	ISP-136	ISP-227	VS-762
Unit	AND	CM	LE	AC	SE	MLN	MC	CA	NU	NU	MCR	PC	MZ
	andesite	trachyte	rhyolite	trachyte	rhyolite	rhyolite	rhyolite	rhyolite	rhyolite	rhyolite	rhyolite	trachyte	rhyolite
Major elements (wt %)													
SiO_2	56.92	62.63	69.24	64.17	70.19	69.30	70.71	71.45	69.76	70.42	69.24	66.61	68.13
TiO_2	0.81	0.83	0.45	0.82	0.40	0.27	0.36	0.27	0.48	0.49	0.64	0.86	0.53
Al_2O_3	17.87	18.09	14.95	16.61	14.91	15.92	14.89	14.77	14.62	15.11	14.90	15.45	15.61
$Fe_2O_3^T$	8.59	6.25	3.59	5.14	3.49	3.02	2.91	2.66	2.60	2.72	3.38	4.74	2.69
MnO	0.17	0.07	0.02	0.05	0.04	0.07	0.05	0.02	0.07	0.03	0.09	0.04	0.05
MgO	2.86	0.49	0.20	0.72	0.23	0.22	0.23	0.36	0.22	0.32	0.77	0.33	0.40
CaO	7.27	2.72	1.14	3.30	1.20	1.64	0.96	0.72	1.11	0.81	0.78	2.21	0.82
Na_2O	2.70	3.55	3.27	3.93	4.16	3.71	3.78	2.93	4.09	3.92	3.31	4.66	4.69
K_2O	1.62	4.00	5.61	4.06	5.14	4.26	5.91	5.80	5.48	5.72	5.78	4.11	5.32
P_2O_5	0.23	0.02	0.03	0.23	0.13	0.05	0.04	0.03	0.08	0.05	0.14	0.24	0.04
LOI	0.38	2.14	1.24	1.09	0.69	1.09	0.77	1.81	0.80	0.96	2.00	1.41	1.43
Total	99.39	100.78	99.73	100.09	100.56	99.52	100.59	100.78	99.29	100.54	101.02	100.64	99.69
Agpaicity index	0.35	0.56	0.77	0.65	0.83	0.67	0.85	0.75	0.87	0.84	0.79	0.78	0.86
Fe_2O_3/FeO*	0.35	0.5	0.5	0.5	0.5	0.5	0.5	0.5	0.5	0.5	0.5	0.5	0.5
Mineral norm (wt %)													
qz	12.19	17.38	23.81	15.85	21.17	25.32	21.38	27.83	20.61	21.43	23.14	16.95	16.50
or	9.84	24.28	34.07	24.47	30.62	25.77	35.22	35.05	32.99	34.12	34.85	24.61	31.87
ab	24.95	32.79	30.21	35.99	37.62	34.15	34.24	26.94	37.42	35.54	30.33	42.42	42.70
an	32.89	13.75	5.62	15.18	5.18	8.01	4.54	3.47	5.08	3.73	3.02	9.28	3.90
crn	-	3.40	1.69	0.33	0.69	2.63	0.68	2.72	0.16	1.23	2.36	-	0.82
di	2.21	-	-	-	-	-	-	-	-	-	-	0.19	-
hyp	14.06	5.09	2.70	4.85	2.75	2.65	2.39	2.68	2.02	2.28	3.98	3.26	2.49
acm	-	-	-	-	-	-	-	-	-	-	-	-	-
mag	2.22	2.09	1.20	1.70	1.14	1.00	0.95	0.88	0.86	0.89	1.12	1.56	0.89
ilm	1.16	1.19	0.64	1.16	0.56	0.38	0.50	0.38	0.68	0.69	0.90	1.22	0.74
ttn	-	-	-	-	-	-	-	-	-	-	-	-	-
ap	0.49	0.04	0.06	0.48	0.26	0.10	0.08	0.05	0.17	0.11	0.30	0.51	0.07
rt	-	-	-	-	-	-	-	-	-	-	-	-	-
NMS	-	-	-	-	-	-	-	-	-	-	-	-	-
%An	56.86	29.54	15.68	29.66	12.10	19.01	11.71	11.40	11.96	9.49	9.04	17.94	8.36

Sample	ISP-209	ISP-254	ANT-57	ISP-150	ISP-179	ANT-110	ISP-75	ISP-247	VS-789	ANT-12	ISP-192	ISP-210
Unit	MZ rhyolite	MZ rhyolite	CO rhyolite	CO rhyolite	MU rhyolite	MU rhyolite	CF rhyolite	CF rhyolite	PA rhyolite	SP rhyolite	PM rhyolite	CL rhyolite
Major elements (wt %)												
SiO_2	69.23	69.70	74.27	75.90	74.59	73.13	73.09	72.93	74.97	70.08	74.08	74.14
TiO_2	0.54	0.53	0.22	0.15	0.18	0.17	0.17	0.29	0.12	0.37	0.11	0.27
Al_2O_3	15.56	15.15	11.31	11.25	12.64	12.76	12.62	13.09	13.36	14.96	14.16	13.42
$Fe_2O_3^T$	2.64	2.74	3.32	2.73	2.50	3.03	2.93	3.37	1.53	2.46	1.29	1.98
MnO	0.05	0.17	0.05	0.05	0.01	0.07	0.05	0.07	0.05	0.02	0.02	0.02
MgO	0.37	0.42	0.14	0.13	0.14	0.12<LL	0.15	0.12<LL	0.17	<LL	0.09<LL	0.09<LL
CaO	0.88	0.75	0.08	0.22	0.14	0.06	0.08	0.11	0.33	0.72	0.32	0.73
Na_2O	4.68	4.19	4.19	4.38	4.37	4.45	4.48	4.54	4.16	4.46	4.00	3.60
K_2O	5.29	5.61	4.77	4.43	5.01	5.03	4.94	5.14	5.03	5.36	5.35	5.35
P_2O_5	0.02	0.03	0.03	0.00<LL	0.04	0.02	0.02	0.03	0.02	0.05	0.01	0.02
LOI	0.62	0.99	0.68	0.52	0.91	0.80	0.62	0.63	1.05	0.48	0.93	0.57
Total	99.86	100.25	99.04	99.74	100.52	99.63	99.12	100.29	100.76	98.95	100.34	100.17
Agpaicity index	0.86	0.86	1.07	1.07	1.00	1.00	1.01	0.99	0.92	0.88	0.87	0.87
Fe_2O_3/FeO*	0.5	0.5	0.5	0.5	0.5	0.5	0.5	0.5	0.5	0.5	0.5	0.5
Mineral norm (wt %)												
qz	17.45	19.56	29.42	31.11	26.98	25.17	25.42	23.78	28.09	20.24	27.28	28.69
or	31.41	33.49	29.00	26.68	29.93	30.29	29.80	30.66	29.93	32.21	31.90	32.05
ab	42.23	37.97	34.59	35.91	39.68	40.67	40.58	41.16	37.66	40.73	36.24	32.76
an	4.26	3.54	-	-	0.06	-	-	0.20	1.53	3.33	1.51	3.54
crn	0.66	1.00	-	-	-	-	-	-	0.58	0.68	1.38	0.49
di	-	-	0.15	0.89	0.30	0.14	0.22	0.13	-	-	-	-
hyp	2.34	2.76	3.38	2.47	1.89	2.45	2.49	2.50	1.52	1.37	1.10	1.40
acm	-	-	2.95	2.40	-	0.01	0.39	-	-	-	-	-
mag	0.86	0.90	-	-	0.82	1.00	0.82	1.10	0.50	0.81	0.42	0.65
ilm	0.75	0.74	0.31	0.21	0.25	0.23	0.23	0.41	0.16	0.52	0.15	0.38
ttn	-	-	-	-	-	-	-	-	-	-	-	-
ap	0.04	0.06	0.06	-	0.08	0.04	0.04	0.06	0.03	0.10	0.02	0.04
rt	-	-	-	-	-	-	-	-	-	-	-	-
NMS	-	-	0.14	0.34	-	-	-	-	-	-	-	-
%An	9.17	8.52	-	-	0.16	-	-	0.48	3.90	7.57	4.01	9.76

Sample	VS-721	VS-786	VS-784	VS-782	VS-783	VS-763	VS-790	VS-788	VS-757	ISP-252	ISP-136	ISP-227	VS-762
Unit	AND andesite	CM trachyte	LE rhyolite	AC trachyte	SE rhyolite	MLN rhyolite	MC rhyolite	CA rhyolite	NU rhyolite	NU rhyolite	MCR rhyolite	PC trachyte	MZ rhyolite
As[4]	na	4.00	23.7	5.37	14.2	2.19	19.0	16.1	12.9	19.7	20.9	9.05	5.56
Ba[2]	401	863	779	890	1100	983	1380	444	1100	1160	996	723	944
Be[4]	na	4.00	4.72	2.14	3.91	2.10	3.11	3.31	3.26	3.29	3.54	3.12	2.53
Bi[4]	na	0.01	0.14	0.01	na	na	0.05	0.17	0.01	0.03	0.01	0.01	0.02
Ce[2]	39.2	65.1	120	89.6	134	86.9	122	162	101	165	96.9	81.0	132
Co[1]	36.2	10.7	8.7	15.2	8.4	23.3	12.1	5.2	26.5	13.6	6.8	21.1	28.8
Cr[3]	<LL	10.4	10.6	12.6	8.08	17.8	8.63	9.84	7.42	7.89	8.68	8.63	18.5
Cs[4]	na	1.67	6.44	3.08	3.40	1.15	4.69	4.63	2.96	4.85	5.22	3.10	2.77
Cu[3]	12.9	9.94	6.51	8.68	4.82	5.15	4.54	5.27	4.44	4.30	5.58	10.8	7.46
Dy[4]	na	5.63	10.4	7.62	8.03	3.55	9.00	9.50	7.72	9.81	7.56	6.12	10.5
Er[4]	na	2.93	5.74	3.95	3.89	1.83	4.69	5.13	4.03	5.02	3.98	3.30	5.35
Eu[4]	na	1.93	1.45	2.03	1.92	0.97	1.77	0.97	1.83	1.96	1.75	1.60	2.20
Ga[1]	19.0	20.6	18.4	19.1	18.6	15.5	16.1	16.5	20.9	16.7	16.9	18.1	21.2
Gd[4]	na	6.70	11.8	9.03	9.81	4.83	10.3	10.8	8.89	11.7	8.58	7.14	12.4
Ge[4]	na	1.17	1.56	1.14	1.51	1.41	1.45	1.34	1.39	1.53	1.45	1.27	1.53
Hf[4]	na	6.44	9.10	6.09	2.40	8.57	5.81	6.55	5.64	7.45	7.37	7.45	5.39
Ho[4]	na	1.00	1.94	1.38	1.38	0.60	1.60	1.73	1.39	1.74	1.36	1.11	1.89
La[4]	na	39.7	65.4	46.9	58.3	45.0	59.5	68.6	56.5	70.7	52.9	44.3	77.3
Li[4]	na	13.2	21.2	17.6	15.8	15.2	16.5	37.7	19.1	18.3	21.0	14.2	25.1
Lu[4]	na	0.39	0.78	0.51	0.45	0.27	0.59	0.68	0.50	0.63	0.54	0.46	0.61
Mo[3]	<LL	1.24	3.10	2.06	2.28	0.26	2.05	1.13	2.81	2.09	2.16	2.48	1.14
Nb[1]	10.6	27.0	28.7	26.1	30.7	19.9	35.2	38.3	42.2	45.7	41.7	46.7	44.0
Nd[4]	na	34.1	62.2	44.6	51.7	29.4	52.6	56.3	47.2	61.8	45.1	36.5	60.9
Ni[3]	<LL	3.83	2.84	3.89	2.11	1.84	2.32	5.73	0.89	1.98	1.72	3.95	2.91
Pb[1]	13.1	22.4	48.7	17.4	22.4	25.2	26.9	27.2	18.8	21.3	24.5	21.9	18.2
Pr[4]	na	8.90	16.4	11.4	13.8	8.67	13.9	15.5	12.8	16.4	12.2	9.78	16.2
Rb[1]	58.5	125	198	127	167	125	202	225	182	204	210	135	174
Sb[4]	na	1.25	2.44	0.74	1.32	0.22	1.63	2.46	1.74	4.19	3.04	1.29	0.99
Sc[4]	na	17.7	11.1	13.6	10.0	3.00	11.8	9.88	7.64	7.55	9.03	7.42	5.29
Sm[4]	na	6.79	12.2	8.91	9.97	4.82	10.3	10.8	8.93	11.5	8.65	6.82	11.5
Sn[2]	2.2	4.9	3.7	2.1	4.1	1.21*	3.4	7.2	4.2	4.4	2.62*	3.3	2.59*
Sr[2]	325	234	96.6	273	127	172	75.3	65.2	108	94.9	81.6	232	118
Ta[4]	na	2.60	1.79	3.92	1.78	0.41	1.84	1.98	3.38	1.26	5.91	6.77	0.39
Tb[4]	na	0.98	1.77	1.32	1.41	0.63	1.52	1.60	1.33	1.70	1.28	1.06	1.83
Te[4]	na	0.18	0.07	0.15	0.08	0.11	0.04	0.05	0.11	0.03	0.06	0.21	0.08
Th[1]	7.50	11.5	22.9	17.1	22.4	15.8	13.2	22.6	15.1	15.6	15.9	10.1	14.9
Tl[4]	na	0.42	0.90	0.55	0.53	0.48	0.99	1.21	0.45	0.58	0.74	0.26	0.26
Tm[4]	na	0.40	0.80	0.55	0.52	0.25	0.64	0.73	0.55	0.67	0.57	0.46	0.69
U[4]	na	2.29	4.40	1.86	1.64	2.31	3.60	4.99	3.62	3.93	3.95	3.11	2.96
V[1]	136	34.1	26.2	50.9	15.1	9.8	16.1	16.9	22.5	21.2	33.8	58.8	20.7
W[1]	185	30.3	78.1	88.5	99.3	68.4	107	47.8	138	144	54.3	129	82.1
Y[1]	22.9	28.2	54.8	39.9	42.4	17.5	51.0	53.8	42.0	52.2	40.5	35.7	63.6
Yb[4]	na	2.65	5.30	3.48	3.30	1.79	4.13	4.68	3.54	4.35	3.74	3.06	4.22
Zn[1]	97.5	80.1	69.2	73.8	74.6	52.9	71.2	95.4	44.4	66.0	89.1	94.1	62.2
Zr[1]	143	318	409	327	410	306	460	304	451	492	454	392	476

Sample	**ISP-209**	**ISP-254**	**ANT-57**	**ISP-150**	**ISP-179**	**ANT-110**	**ISP-75**	**ISP-247**	**VS-789**	**ANT-12**	**ISP-192**	**ISP-210**
Unit	MZ rhyolite	MZ rhyolite	CO rhyolite	CO rhyolite	MU rhyolite	MU rhyolite	CF rhyolite	CF rhyolite	PA rhyolite	SP rhyolite	PM rhyolite	CL rhyolite
As	6.46	10.6	3.32	1.53	4.21	5.50	na	4.22	4.90	4.96	2.44	5.19
Ba	1230	1090	25.5*	2.59*	34.4*	15.8*	<LL	122	40.5	786	49.9*	507
Be	2.76	3.17	6.81	7.90	6.03	6.06	na	4.26	3.66	3.18	2.69	3.29
Bi	0.01	0.05	0.02	na	0.01	0.01	na	0.02	0.01	0.05	0.01	0.02
Ce	126	113	236	214	227	132	173	165	106	106	100	91.0
Co	17.1	16.1	25.6	34.9	19.5	28.3	20.3	13.7	15.3	17.7	14.3	21.8
Cr	17.5	7.60	6.86	18.3	7.41	7.50	<LL	7.47	7.48	7.36	18.0	7.73
Cs	3.04	5.03	2.11	4.58	3.42	2.83	na	2.62	3.73	1.62	2.67	4.22
Cu	5.10	15.2	2.80	2.27	2.29	2.50	<LL	3.35	3.08	3.69	2.55	3.69
Dy	9.20	12.7	16.2	19.2	18.8	11.9	na	12.0	5.17	5.14	7.75	5.71
Er	4.57	6.43	8.96	11.5	9.44	6.40	na	6.07	2.91	2.49	4.42	3.19
Eu	2.34	2.39	0.42	0.09	0.40	0.15	na	0.60	0.23	1.08	0.32	0.73
Ga	15.3	16.8	24.7	23.8	23.8	23.1	22.8	20.2	15.4	16.1	16.6	14.7
Gd	10.8	14.3	17.1	18.2	21.2	13.3	na	13.8	5.94	6.63	8.77	6.82
Ge	1.46	1.48	2.00	2.37	1.80	1.93	na	1.70	1.55	1.40	1.40	1.21
Hf	5.98	2.94	21.2	24.2	7.68	12.2	na	5.33	4.18	5.43	4.86	3.41
Ho	1.57	2.23	2.96	3.72	3.28	2.22	na	2.12	0.95	0.86	1.47	1.07
La	66.5	81.8	105	91.9	118	89.7	na	81.2	51.0	54.2	68.5	56.2
Li	14.5	15.9	19.4	64.4	21.0	21.9	na	11.0	14.9	5.93	11.1	10.1
Lu	0.55	0.76	1.29	1.65	1.22	0.81	na	0.77	0.44	0.31	0.57	0.42
Mo	1.29	2.22	1.38	0.59	1.33	1.59	<LL	1.69	1.69	3.86	0.67	1.44
Nb	43.7	43.3	107	105	90.9	88.9	87.3	78.3	39.7	41.0	35.1	26.4
Nd	56.4	80.4	85.8	79.6	105	71.2	na	71.7	31.9	37.5	46.1	35.7
Ni	1.45	2.75	0.57	0.64	2.21	2.19	<LL	2.02	2.63	0.70	2.27	1.56
Pb	20.1	18.4	24.1	30.8	27.2	27.6	21.1	22.3	69.7	15.6	19.6	31.5
Pr	15.1	21.5	23.7	22.2	27.4	19.8	na	19.4	9.50	11.0	13.1	10.0
Rb	168	184	214	286	223	221	208	189	198	152	191	211
Sb	0.84	1.22	0.38	0.65	0.60	0.54	na	0.71	0.86	0.51	0.31	0.35
Sc	5.37	7.64	2.02	2.62	4.02	3.80	na	5.83	1.68	4.39	1.77	1.73
Sm	10.9	15.1	16.3	17.1	21.0	13.1	na	13.7	5.58	6.70	8.22	6.17
Sn	2.12*	5.7	6.7	8.7	6.9	6.8	7.2	5.5	3.7	1.9	1.07*	0.90*
Sr	127	120	9.05*	4.26*	22.3*	7.49*	24.8	22.7*	12.6*	77.1	11.9*	87.8
Ta	0.16	1.52	13.2	0.87	4.05	7.47	na	2.82	3.94	3.49	0.25	3.43
Tb	1.57	2.16	2.69	3.09	3.23	2.00	na	2.04	0.87	0.92	1.31	0.98
Te	0.12	0.07	0.09	0.10	0.02	0.02	na	0.06	0.07	0.06	0.05	0.08
Th	12.1	14.0	20.4	20.1	16.2	16.6	16.7	13.0	24.0	22.8	23.7	26.9
Tl	1.48	0.78	0.42	0.51	0.73	0.65	na	0.25	0.17	0.41	0.38	0.10
Tm	0.61	0.87	1.28	1.69	1.28	0.86	na	0.83	0.43	0.33	0.61	0.45
U	3.10	2.73	2.02	7.98	4.27	4.47	na	3.49	3.95	2.77	4.06	3.72
V	20.9	25.1	10.1	7.0	10.3	8.5	8.8	9.4	7.5	18.0	9.6	16.7
W	145	107	245	346	137	179	155	136	83.6	141	94.3	189
Y	45.9	73.9	74.9	99.8	99.3	75.8	68.1	68.2	29.6	25.8	43.1	37.5
Yb	3.86	5.52	8.67	11.3	8.29	5.42	na	5.31	2.90	2.19	3.91	2.89
Zn	62.4	81.1	118	156	116	127	98.1	91.9	111	37.6	58.6	49.6
Zr	475	451	791	825	696	654	656	585	201	415	261	234

3. ANALYSIS OF Sr, Nd AND Pb ISOTOPE RATIOS

Samples for Sr and Nd isotope analysis were dissolved in $HF+HNO_3$, dried in HNO_3 and HCl, and brought into solution in HCl. Sr and REE were separated using DOVEX AG-50x8 (200-400 mesh) cation exchange resin, and Nd was separated using hydrogen di-ethylhexyl-phosphate (HDEHP)-coated resin. Samples for Pb isotope analysis were dissolved in $HF+HNO_3$, dried in HNO_3 and HCl, and brought into solution in HBr; lead separation was performed in Bio-Rad 10-ml polyethylene columns with Dowex AG1-8X anion resin, using 1N HBr to elute other elements and 6N HCl to elute Pb.

Sr and Nd isotope ratios were determined using a VG-Micromass Sector 54 TIMS with 5 Faraday cups in multi-dynamic mode. $^{87}Sr/^{86}Sr$ measurements were corrected for ^{87}Rb interferences and normalized to $^{88}Sr/^{86}Sr = 0.1194$ for mass fractionation. $^{143}Nd/^{144}Nd$ measurements were corrected for ^{142}Ce and ^{144}Sm interferences, and normalized to $^{146}Nd/^{144}Nd = 0.7219$ for mass fractionation. During the run period two isotopic reference samples (NIST SRM 987 for Sr and La Jolla for Nd) were repeatedly analysed. Unknowns were normalized to the long term average values of the laboratory, which were $^{87}Sr/^{86}Sr = 0.710248 \pm 0.000050$ (2σ, n=722) for NIST SRM 987 and $^{143}Nd/^{144}Nd = 0.511848 \pm 0.000030$ (2σ, n=140) for La Jolla.

Pb isotopic ratios were determined using a Thermo-Finnigan Triton TIMS. All runs were corrected for mass fractionation using international standard NIST SRM 981 and values reported by Todt *et al.* (1996). Long term relative 2σ of repeated standards measured over the 2 months period prior to the analysis are 0.04 % ($^{206}Pb/^{204}Pb$), 0.06 % ($^{207}Pb/^{204}Pb$), 0.08 % ($^{208}Pb/^{204}Pb$), 0.02 % ($^{207}Pb/^{206}Pb$) and 0.04 % ($^{208}Pb/^{206}Pb$).

References:

Todt, W., Cliff, R., Hanser, A., Hofmann, A., 1996. Evaluation of a ^{202}Pb-^{205}Pb double spike for high-precision lead isotope analysis. Geophysical Monograph Series 95, 429-437.

Sample	Unit	$^{87}Sr/^{86}Sr$	$^{143}Nd/^{144}Nd$	$^{206}Pb/^{204}Pb$	$^{207}Pb/^{204}Pb$	$^{208}Pb/^{204}Pb$	Age (Ma)	Rb	Sr	$^{87}Sr/^{86}Sr_i$
VS 721	AND	0.707533 ± 0.000004	0.512355 ± 0.000004	18.5697 ±0.0005	15.6757 ± 0.0005	38.7462 ±0.0017	18	59	325	0.707399
VS 786	1 (CM)	0.707863 ± 0.000007	0.512450 ± 0.000005	18.7249 ±0.0005	15.6961 ± 0.0005	38.9038 ±0.0017	16.5	125	234	0.707569
VS 784	2 (LE)	0.709245 ± 0.000005	0.512471 ± 0.000004	18.4636 ±0.0002	15.6950 ± 0.0004	38.6547 ±0.0010	16.5	198	96.6	0.708273
VS 782	3 (AC)	0.706916 ± 0.000005	0.512495 ± 0.000003	18.7180 ±0.0005	15.6877 ± 0.0005	38.8761 ±0.0015	16.5	127	273	0.706646
VS 783	4 (SE)	0.707662 ± 0.000005	0.512506 ± 0.000003	18.7187 ±0.0008	15.6829 ± 0.0010	38.8718 ±0.0031	16.5	167	127	0.706901
VS 763	5 (MLN)	0.707267 ± 0.000006	0.512453 ± 0.000004	18.7089 ±0.0003	15.6763 ± 0.0003	38.8647 ±0.0007	15.5	125	172	0.706776
VS 790	6 (MC)	0.709708 ± 0.000006	0.512510 ± 0.000004	18.7199 ±0.0006	15.6793 ± 0.0005	38.8182 ±0.0013	15.5	202	75.3	0.708077
VS 788	7 (CA)	0.710482 ± 0.000006	0.512472 ± 0.000006	18.7186 ±0.0003	15.6721 ± 0.0002	38.7995 ±0.0006	15.5	225	65.2	0.707830
VS 757	8 (NU)	0.708074 ± 0.000005	0.512535 ± 0.000004	18.7706 ±0.0004	15.6999 ± 0.0004	38.9282 ±0.0012	15.5	182	108	0.706949
ISP 252	8 (NU)	0.708544 ± 0.000005	0.512543 ± 0.000003	18.7785 ±0.0008	15.7098 ± 0.0007	38.9594 ±0.0018	15.5	204	94.9	0.707419
ISP 227	9 (PC)	0.705482 ± 0.000006	0.512649 ± 0.000003	18.8000 ±0.0020	15.7044 ± 0.0023	38.9601 ±0.0080	15	135	232	0.705170
ISP 136	10 (MCR)	0.708877 ± 0.000005	0.512535 ± 0.000005	18.7631 ±0.0018	15.6960 ± 0.0020	38.9017 ±0.0068	15	210	81.6	0.707356
VS 762	11 (MZ)	0.707192 ± 0.000007	0.512614 ± 0.000004	18.7252 ±0.0040	15.6930 ± 0.0040	38.8586 ±0.0120	15	174	118	0.706224
ISP 209	11 (MZ)	0.707206 ± 0.000006	0.512556 ± 0.000004	18.7811 ±0.0004	15.6911 ± 0.0004	38.9119 ±0.0014	15	168	127	0.706334
ISP 254	11 (MZ)	0.707574 ± 0.000006	0.512649 ± 0.000006	18.7876 ±0.0006	15.6931 ± 0.0006	38.9217 ±0.0020	15	184	120	0.706455
ANT 57	12 (CO)	0.729451 ± 0.000005	0.512694 ± 0.000003	18.9018 ±0.0017	15.7220 ± 0.0020	39.1431 ±0.0070	15	214	9.05	0.713501
ISP 150	12 (CO)	0.754174 ± 0.000005	0.512685 ± 0.000003	18.8737 ±0.0007	15.6870 ± 0.0006	38.9851 ±0.0017	15	286	4.26	0.709799
ANT 110	13 (MU)	0.731066 ± 0.000004	0.512618 ± 0.000003	18.8684 ±0.0002	15.6848 ± 0.0002	38.9921 ±0.0006	15	221	7.49	0.710925
ISP 179	13 (MU)	0.717596 ± 0.000006	0.512624 ± 0.000004	18.8519 ±0.0003	15.6593 ± 0.0003	38.9085 ±0.0009	15	223	22.3	0.711110
ISP 71	14 (CF)	0.716069 ± 0.000006	0.512706 ± 0.000004	18.8549 ±0.0017	15.6680 ± 0.0020	38.9429 ±0.0070	15	161	18.5	0.710342
ISP 75	14 (CF)	0.716736 ± 0.000005	0.512608 ± 0.000004	18.9000 ±0.0042	15.7216 ± 0.0050	39.1180 ±0.0016	15	208	24.8	0.710094
ISP247	14 (CF)	0.714227 ± 0.000005	0.512619 ± 0.000005	18.7359 ±0.0003	15.6648 ± 0.0003	38.8111 ±0.0007	15	189	22.72	0.708810
VS 789	15 (PA)	0.717806 ± 0.000006	0.512672 ± 0.000003	18.2394 ±0.0028	15.6557 ± 0.0034	38.3115 ±0.0130	15	198	12.6	0.707183
ANT 12	16 (SP)	0.706611 ± 0.000006	0.512693 ± 0.000003	18.8711 ±0.0040	15.6949 ± 0.0040	39.0060 ±0.0140	15	152	77.1	0.705255
ISP 192	17 (PM)	0.717585 ± 0.000006	0.512596 ± 0.000003	18.8509 ±0.0007	15.7013 ± 0.0007	39.0618 ±0.0012	15	191	11.9	0.706641
ISP 210	18/19 (CL/PG)	0.707526 ± 0.000005	0.512590 ± 0.000005	18.7803 ±0.0003	15.6638 ± 0.0004	38.8738 ±0.0012	15	211	87.8	0.706186

Isotopic composition of representative samples of Sulcis Oligo-Miocene volcanism obtained in this study. $^{87}Sr/^{86}Sr_i$: initial $^{87}Sr/^{86}Sr$. Ages shown are those used for age correction. Rb and Sr concentrations in µg/g.

4. ORIGIN OF LITERATURE GEOCHEMICAL DATA

	M&T	Isotope ratios		
		Sr	Nd	Pb
OLIGO-MIOCENE MAGMATISM				
Arcuentu				
Brotzu *et al.* (1997a)	x			
Downes *et al.* (2001)	x	x	x	
Franciosi *et al.* (2003)	x	x	x	x
Lustrino *et al.* (2004)	x	x	x	
Lustrino *et al.* (2009)	x			
Lustrino *et al.* (2013)	x	x	x	x
Logudoro-Bossano				
Coulon (1977)	x			
Lustrino *et al.* (2004)	x	x		
Lustrino *et al.* (2013)	x	x	x	x
Marmilla				
Lustrino *et al.* (2013)	x	x	x	x
Montresta				
Morra *et al.* (1997)	x	x		
Franciosi *et al.* (2003)	x	x	x	x
Lustrino *et al.* (2004)	x	x	x	x
Lustrino *et al.* (2009)	x			
Lustrino *et al.* (2013)	x	x	x	x
Sarroch				
Conte (1997)	x			
Sindia				
Lonis *et al.* (1997)	x	x		
Lustrino *et al.* (2004)	x	x		
Sulcis				
Morra *et al.* (1994)	x	x		
Brotzu *et al.* (1997b)	x	x		
Conte *et al.* (2010)	x	x		
Lustrino *et al.* (2013)	x	x	x	x
Villanovaforru				
Mattioli *et al.* (2000)	x			
Isola del Toro*				
Lustrino *et al.* (2007a)	x	x	x	
Lustrino *et al.* (2013)	x	x	x	x
Other OM				
Guarino *et al.* (2011)	x			
Lustrino *et al.* (2009)	x			
Lustrino *et al.* (2013)	x	x	x	x

	M&T	Isotope ratios		
		Sr	Nd	Pb
PLIO-PLEISTOCENE MAGMATISM				
Other than Monte Arci				
Lustrino *et al.* (1996)	x			
Lustrino (2000)	x			
Lustrino *et al.* (2000)	x	x	x	x
Lustrino *et al.* (2002)	x	x	x	x
Lustrino *et al.* (2004)	x	x	x	x
Lustrino *et al.* (2007b)	x	x	x	
Fedele *et al.* (2007)	x	x	x	
Rutter (1987)	x	x		
Lustrino *et al.* (2013)	x	x	x	x
Monte Arci				
Cioni *et al.* (1982)	x	x		
Dostal *et al.* (1982b)	x			
Montanini & Meli (1992)	x			
Montanini *et al.* (1994)	x	x	x	
Lustrino *et al.* (2013)	x	x	x	x
OTHER COMPONENTS				
Sardinian continental crust				
Rutter (1987)	x	x		
Caggianelli *et al.* (1991)	x	x	x	x
Rottura *et al.* (1991)	x	x	x	x
Francalanci *et al.* (1993)	x			x
Tommasini *et al.* (1995)	x	x	x	
Oceanic sediment				
White *et al.* (1985)	T	x	x	x
Othman *et al.* (1989)	T	x	x	x
Plank & Langmuir (1998)	x	x	x	x
Carpathians				
Harangi *et al.* (2007)	x	x	x	x
Eolian Islands				
Ellam *et al.* (1989)	x	x	x	x
Francalanci *et al.* (1993)	x	x	x	x
Del Moro *et al.* (1998)	x	x	x	x
Mantle end-members				
Hart *et al.* (1992)		x	x	x
EAR-like mantle				
<u>Component C</u>				
Stracke *et al.* (2005)		x	x	x
Cadoux *et al.* (2007)		x	x	x
<u>EAR</u>				
Granet *et al.* (1995)		x	x	x
Wilson & Bianchini (1999)		x	x	x
<u>LVC</u>				
Hoernle *et al.* (1995)		x	x	x

Origin and available data of literature geochemical data used in this work. *Isola del Toro samples are presented in Oligo-Miocene magmatism following conclusions of this study, but in Discussion diagrams they are presented together with RPV Plio-Pleistocene lavas following prior classification. M&T: major and trace elements; EAR: European Asthenospheric Reservoir; LVC: Low Velocity Component.

References:

Brotzu, P., Lonis, R., Melluso, L., Morbidelli, L., Traversa, G., Franciosi, L., 1997a. Petrology and evolution of calcalkaline magmas from the Arcuentu volcanic complex (SW Sardinia, Italy). Periodico di Mineralogia 66, 151-184.

Brotzu, P., Callegari, E., Morra, V., Ruffini, R., 1997b. The orogenic basalt-andesite suites from the Tertiary volcanic complex of Narcao, SW-Sardinia (Italy): petrology, geochemistry and Sr-isotope characteristics. Periodico di Mineralogia 66, 101-150.

Cadoux, A., Blichert-Toft, J., Pinti, D.L., Albarede, F., 2007. A unique lower mantle source for Southern Italy volcanics. Earth and Planetary Science Letters 259, 227-238.

Caggianelli, A., Del Moro, A., Paglionico, A., Piccarreta, G., Pinarelli, L., Rottura, A., 1991. Lower crustal granite genesis connected with chemical fractionation in the continental crust of Calabria (southern Italy). European Journal of Mineralogy 3, 159-180.

Cioni, R., Clocchiatti, R., Dipaola, G.M., Santacroce, R., Tonarini, S., 1982. Miocene calc-alkaline heritage in the Pliocene post-collisional volcanism of Monte Arci (Sardinia, Italy). Journal of Volcanology and Geothermal Research 14, 133-167.

Conte, A.M., 1997. Petrology and geochemistry of Tertiary calcalkaline magmatic rocks from the Sarroch district (Sardinia, Italy). Periodico di Mineralogia 66, 63-100.

Conte, A.M., Palladino, D.M., Perinelli, C., Argenti, E., 2010. Petrogenesis of the High-Alumina Basalt-Andesite suite from Sant'Antioco Island, SW Sardinia, Italy. Periodico di Mineralogia 79, 27-55.

Coulon, C., 1977. Le volcanisme calco-alcalin cénozoïque de Sardaigne (Italie). Petrographie, géochimie et génèse des laves andesitiques et des ignimbrites. Signification géodynamique. University of Aix-Marseille III, p. 288.

Del Moro, A., Gioncada, A., Pinarelli, L., Sbrana, A., Joron, J.L., 1998. Sr, Nd, and Pb isotope evidence for open system evolution at Vulcano, Aeolian Arc, Italy. Lithos 43, 81-106.

Dostal, J., Dupuy, C., Venturelli, G., 1982b. Geochemistry of volcanic rocks from the Monte Arci (West Sardinia, Italy). Chemical Geology 35, 247-264.

Downes, H., Thirlwall, M.F., Trayhorn, S.C., 2001. Miocene subduction-related magmatism in southern Sardinia: Sr-Nd- and oxygen isotopic evidence for mantle source enrichment. Journal of Volcanology and Geothermal Research 106, 1-21.

Ellam, R.M., Hawkesworth, C.J., Menzies, M.A., Rogers, N.W., 1989. The volcanism of southern Italy: role of subduction and the relationship between potassic and sodic alkaline magmatism. Journal of Geophysical Research-Solid Earth and Planets 94, 4589-4601.

Fedele, L., Lustrino, M., Melluso, L., Morra, V., D'Amelio, F., 2007. The Pliocene Montiferro, volcanic complex (central-western Sardinia, Italy): geochemical observations and petrological implications. Periodico di Mineralogia 76, 101-136.

Francalanci, L., Taylor, S.R., McCulloch, M.T., Woodhead, J.D., 1993. Geochemical and isotopic variations in the calc-alkaline rocks of Aeolian Arc, southern Tyrrhenian Sea, Italy: Constraints on magma genesis. Contributions to Mineralogy and Petrology 113, 300-313.

Franciosi, L., Lustrino, M., Melluso, L., Morra, V., D'Antonio, M., 2003. Geochemical characteristics and mantle sources of the Oligo-Miocene primitive basalts from Sardinia: The role of subduction components. Ofioliti 28, 105-114.

Granet, M., Wilson, M., Achauer, U., 1995. Imaging a mantle plume beneath the French Massif Central. Earth and Planetary Science Letters 136, 281-296.

Guarino, V., Fedele, L., Franciosi, L., Lonis, R., Lustrino, M., Marrazzo, M., Melluso, L., Morra, V., Rocco, I., Ronga, F., 2011. Mineral compositions and magmatic evolution of the calcalkaline rocks of northwestern Sardinia, Italy. Periodico di Mineralogia 80, 517-545.

Harangi, S., Downes, H., Thirlwall, M., Gmeling, K., 2007. Geochemistry, petrogenesis and geodynamic relationships of Miocene calc-alkaline volcanic rocks in the western Carpathian arc, eastern central Europe. Journal of Petrology 48, 2261-2287.

Hart, S.R., Hauri, E.H., Oschmann, L.A., Whitehead, J.A., 1992. Mantle plumes and entrainment - Isotopic evidence. Science 256, 517-520.

Hoernle, K., Zhang, Y.S., Graham, D., 1995. Seismic and geochemical evidence for large-scale mantle upwelling beneath the eastern Atlantic and western and central Europe. Nature 374, 34-39.

Lonis, R., Morra, V., Lustrino, M., Melluso, L., Secchi, F., 1997. Plagioclase textures, mineralogy and petrology of Tertiary orogenic volcanic rocks from Sindia (central Sardinia). Periodico di Mineralogia 66, 185-210.

Lustrino, M., 2000. Petrogenesis of tholeiitic volcanic rocks from central-southern Sardinia. Mineralogica et Petrographica Acta 43, 49-64.

Lustrino, M., Melluso, L., Morra, V., Secchi, F., 1996. Petrology of Plio-Quaternary volcanic rocks from central Sardinia. Periodico di Mineralogia 65, 275-287.

Lustrino, M., Melluso, L., Morra, V., 2000. The role of lower continental crust and lithospheric mantle in the genesis of Plio-Pleistocene volcanic rocks from Sardinia (Italy). Earth and Planetary Science Letters 180, 259-270.

Lustrino, M., Melluso, L., Morra, V., 2002. The transition from alkaline to tholeiitic magmas: a case study from the Orosei-Dorgali Pliocene volcanic district (NE Sardinia, Italy). Lithos 63, 83-113.

Lustrino, M., Morra, V., Meelluso, M., Brotzu, P., D'Amelio, F., Fedele, L., Franciosi, F., Lonis, R., Petteruti Liebercknecht, A.M., 2004. The Cenozoic igneous activity of Sardinia. Periodico di Mineralogia 73, 105-134.

Lustrino, M., Morra, V., Fedele, L., Serracino, M., 2007a. The transition between 'orogenic' and 'anorogenic' magmatism in the western Mediterranean area: the Middle Miocene volcanic rocks of Isola del Toro (SW Sardinia, Italy). Terra Nova 19, 148-159.

Lustrino, M., Melluso, L., Morra, V., 2007b. The geochemical peculiarity of "Plio-Quaternary" volcanic rocks of Sardinia in the circum-Mediterranean Cenozoic Igneous Province, in: Beccaluva, L., Bianchini, G., Wilson, M. (Eds.), Cenozoic volcanism in the Mediterranean area. Geological Society of America Special Paper, pp. 277-301.

Lustrino, M., Morra, V., Fedele, L., Franciosi, L., 2009. Beginning of the Apennine subduction system in central western Mediterranean: Constraints from Cenozoic "orogenic'' magmatic activity of Sardinia, Italy. Tectonics 28, 23.

Lustrino, M., Fedele, L., Melluso, L., Morra, V., Ronga, F., Geldmacher, J., Duggen, S., Agostini, S., Cucciniello, C., Franciosi, L., Meisel, T., 2013. Origin and evolution of Cenozoic magmatism of Sardinia (Italy). A combined isotopic (Sr-Nd-Pb-O-Hf-Os) and petrological view. Lithos 180, 138-158.

Mattioli, M., Guerrera, F., Tramontana, M., Raffaelli, G., D'Atri, M., 2000. High-Mg Tertiary basalts in Southern Sardinia (Italy). Earth and Planetary Science Letters 179, 1-7.

Montanini, A., Meli, S., 1992. Mineralogy and petrology of the mafic inclusion-bearing trachytes from Mt. Arci volcanic massif (Western Sardinia). Neues Jahrbuch Fur Mineralogie-Abhandlungen 164, 139-168.

Montanini, A., Barbieri, M., Castorina, F., 1994. The role of fractional crystallisation, crustal melting and magma mixing in the petrogenesis of rhyolites and mafic inclusion-bearing dacites from the Monte Arci volcanic complex (Sardinia, Italy). Journal of Volcanology and Geothermal Research 61, 95-120.

Morra, V., Secchi, F.A., Assorgia, A., 1994. Petrogenetic significance of peralkaline rocks from Cenozoic calc-alkaline volcanism from Sardinia, Italy. Chemical Geology 118, 109-142.

Morra, V., Secchi, F.A.G., Melluso, L., Franciosi, L., 1997. High-Mg subduction-related tertiary basalts in Sardinia, Italy. Lithos 40, 69-91.

Othman, D.B., White, W.M., Patchett, J., 1989. The geochemistry of marine sediments, island arc magma genesis, and crust-mantle recycling. Earth and Planetary Science Letters 94, 1-2121.

Plank, T., Langmuir, C.H., 1998. The chemical composition of subducting sediment and its consequences for the crust and mantle. Chemical Geology 145, 325-394.

Rottura, A., Del Moro, A., Pinarelli, L., Petrini, R., Peccerillo, A., Caggianelli, A., Bargossi, G.M., Piccarreta, G., 1991. Relationships between intermediate and acidic rocks in orogenic granitoid suites: petrological, geochemical and isotopic (Sr, Nd, Pb) data from Capo Vaticano (southern Calabria, Italy). Chemical Geology 92, 153-176.

Rutter, M.J., 1987. Evidence for crustal assimilation by turbulently convecting, mafic alkaline magmas: geochemistry of mantle xenolith-bearing lavas from northern Sardinia. Journal of Volcanology and Geothermal Research 32, 343-354.

Stracke, A., Hofmann, A.W., Hart, S.R., 2005. FOZO, HIMU, and the rest of the mantle zoo. Geochemistry Geophysics Geosystems 6.

Tommasini, S., Poli, G., Halliday, A.N., 1995. The role of sediment subduction and crustal growth in Hercynian plutonism - isotopic and trace-element evidence from the Sardinia-Corsica batholith. Journal of Petrology 36, 1305-1332.

White, W.M., Dupre, B., Vidal, P., 1985. Isotope and trace element geochemistry of sediments from the Barbados Ridge-Demerara Plain region, Atlantic Ocean. Geochimica Et Cosmochimica Acta 49, 1875-1886.

Wilson, M., Bianchini, G., 1999. Tertiary-Quaternary magmatism within the Mediterranean and surrounding regions, in: Durand, B., Jolivet, L., Horváth, F., Séranne, M. (Eds.), The Mediterranean basins: Tertiary extension within the Alpine Orogen. Geological Society, London, pp. 141-168.

5. COMPLEMENTARY DIAGRAMS

Fig. S1. Harker diagrams of major elements versus silica content, normalized to anhydrous 100 wt %. FeO* is total iron. Concentrations in wt %. White arrows indicate possible evolution trends. Symbols follow Fig. 4.

Fig. S2. Comparison between measured (grey) and age corrected (coloured) isotope ratios in studied samples ordered stratigraphically. Differences between age corrected and measured values are the largest for $^{87}Sr/^{86}Sr$. In the other isotope systems difference is not significant in terms of data interpretation. Thus, age corrected data are only used for the Sr isotope system. Symbols follow Fig. 4.

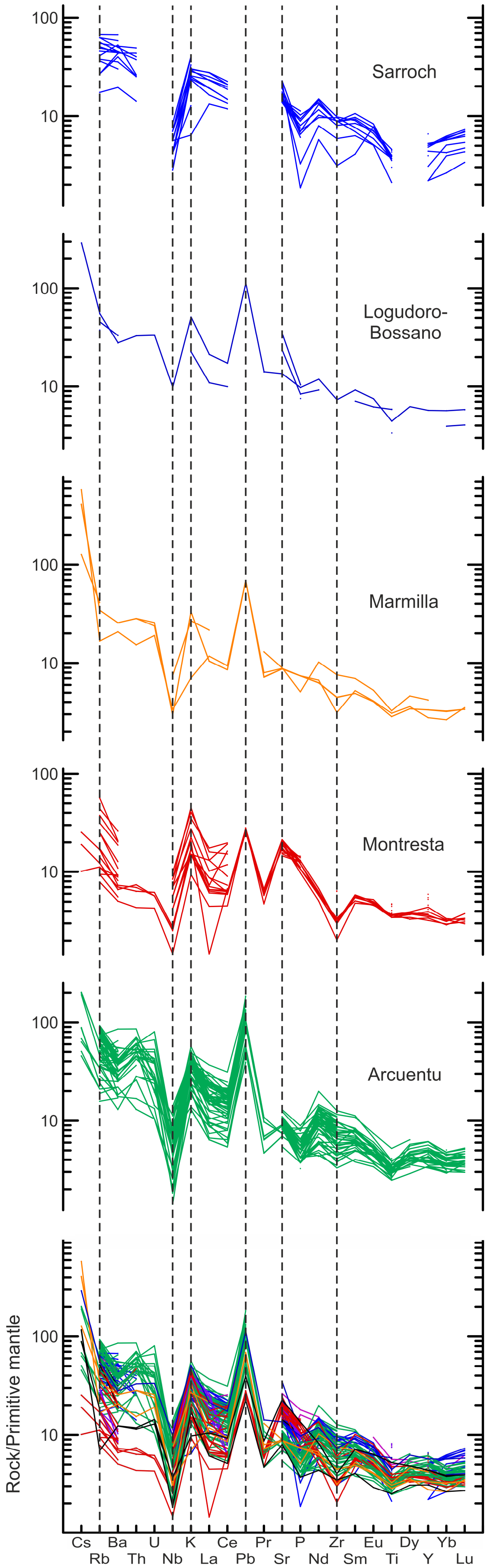

Fig. S3. Trace element multielemental diagrams (normalizing values of Sun & McDonough 1989) of the Oligo-Miocene volcanic rocks of Sardinia with MgO>5 wt %. All the suites are depicted together in the bottom plot while some of the best characterized suites are depicted individually above. All the suites show similar arc-type signatures.

Reference:

Sun, S.S., McDonough, W.F., 1989. Chemical and isotopic systematics of oceanic basalts; implications for mantle composition and processes, in: Saunders, A.D., Norry, M.J. (Eds.), Magmatism in the ocean basins. Geological Society of London, London, pp. 313-435.

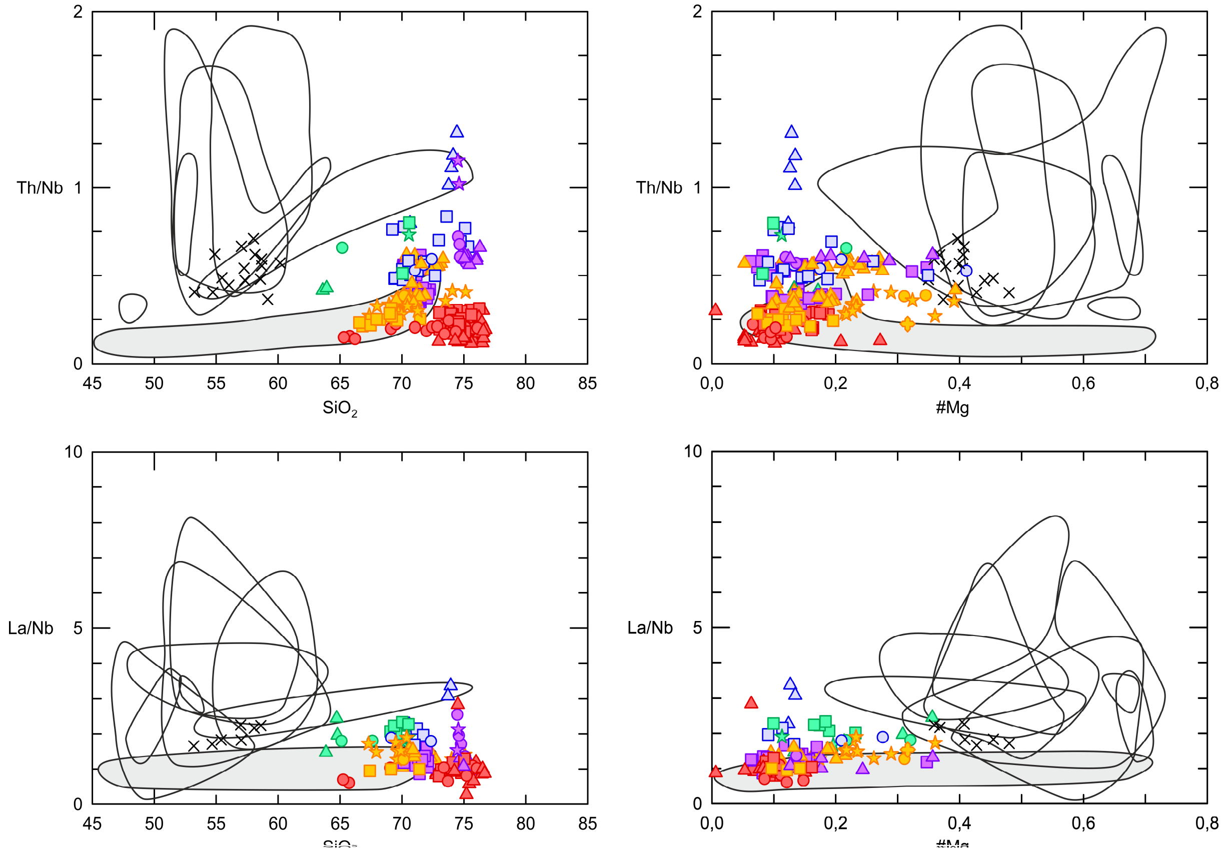

Fig. S4. Th/Nb and La/Nb ratios versus SiO_2 and Mg#. Empty areas represent OM suites. Solid grey area represents PP rocks. Lack of correlation between Th/Nb and La/Nb ratios with AFC indicators (e.g. SiO_2, Mg#) indicates that the subduction signature of most OM rocks was not introduced by crustal assimilation. In the Th/Nb vs. SiO_2 diagram, the OM suite showing correlation is the Arcuentu suite, which also shows clear crustal assimilation trends in isotope space. Symbols follow Fig. 4.

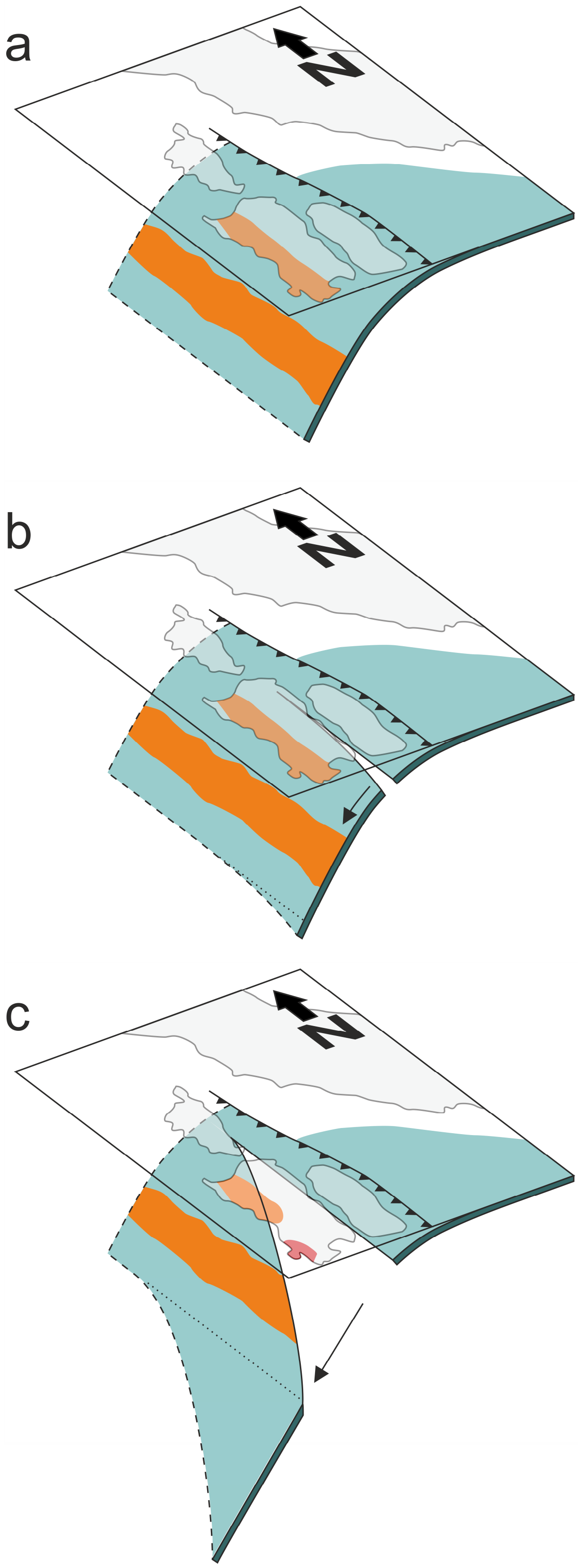

Fig. S5. Schematic diagram of the proposed hypothesis on the evolution of the subduction under Sardinia at the end of the Oligo-Miocene (OM) magmatic cycle. Orange area on the slab represents the zone of fluid release and subduction-controlled calc-alkaline magma production. Orange area on the upper plate is the zone where calc-alkaline volcanism in Sardinia occurs. Red area on the upper plate represents the extension-controlled mildly alkaline and peralkaline magmatism in Sulcis. (**a**) During most of the OM cycle calc-alkaline magmas erupted in western Sardinia, including the Sulcis area. (**b**) Towards the end of the cycle the slab began to tear northwards, parallel to the trench, south of Sardinia. (**c**) In Sulcis, the opening of a slab window may have reduced the input of slab fluids, thus triggering the transition from calc-alkaline to mildly alkaline magmatism as melting continued by decompression due to the existing extensional setting, and possibly also due to the thermal effect of the asthenospheric mantle upwelling through the slab window. During this stage, calc-alkaline and mildly alkaline magmas erupted contemporaneously in northern and southern Sardinia respectively.

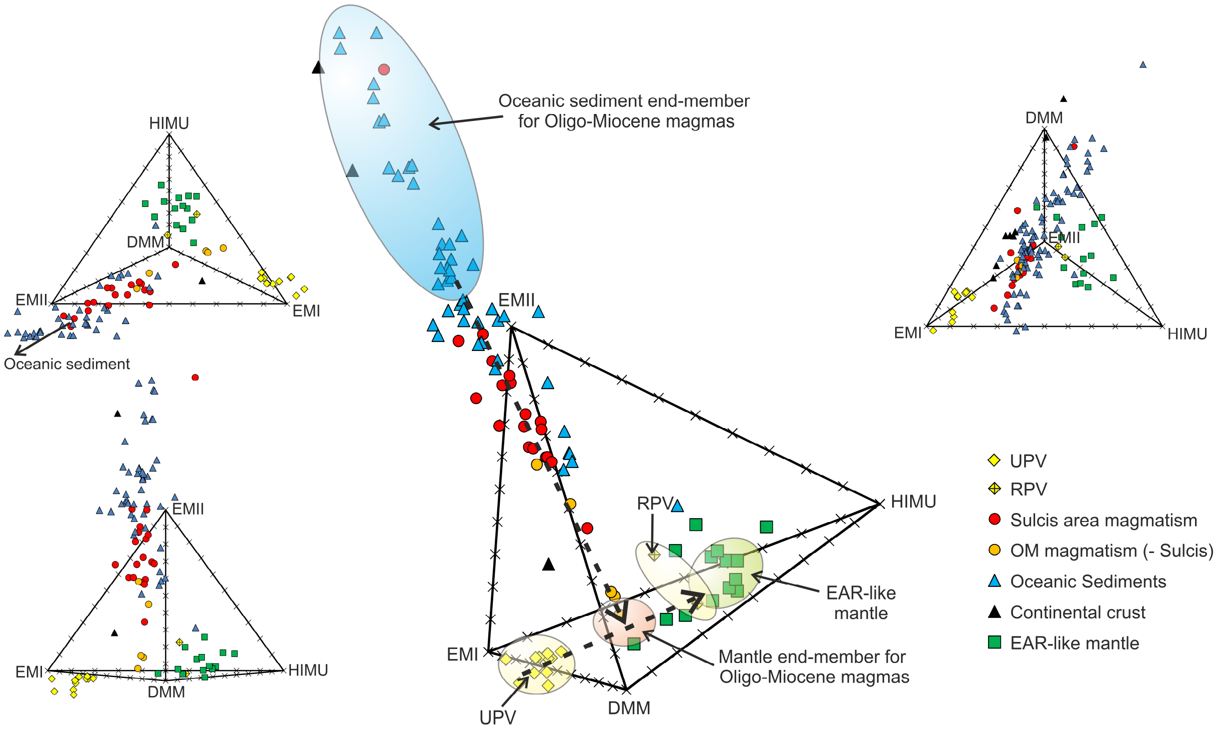

Fig. S6 Tetrahedral diagram (Armienti & Gasperini 2007; Armienti & Longo 2011) based on Sr, Nd and Pb isotope ratios, with endmember mantle components from Hart *et al.* (1992) and Armienti & Gasperini (2007).

References:

Armienti, P., Gasperini, D., 2007. Do we really need mantle components to define mantle composition? Journal of Petrology 48, 693-709.

Armienti, P., Longo, P., 2011. Three-dimensional representation of geochemical data from a multidimensional compositional space. International Journal of Geosciences 2, 231-239.

Hart, S.R., Hauri, E.H., Oschmann, L.A., Whitehead, J.A., 1992. Mantle plumes and entrainment - Isotopic evidence. Science 256, 517-520.

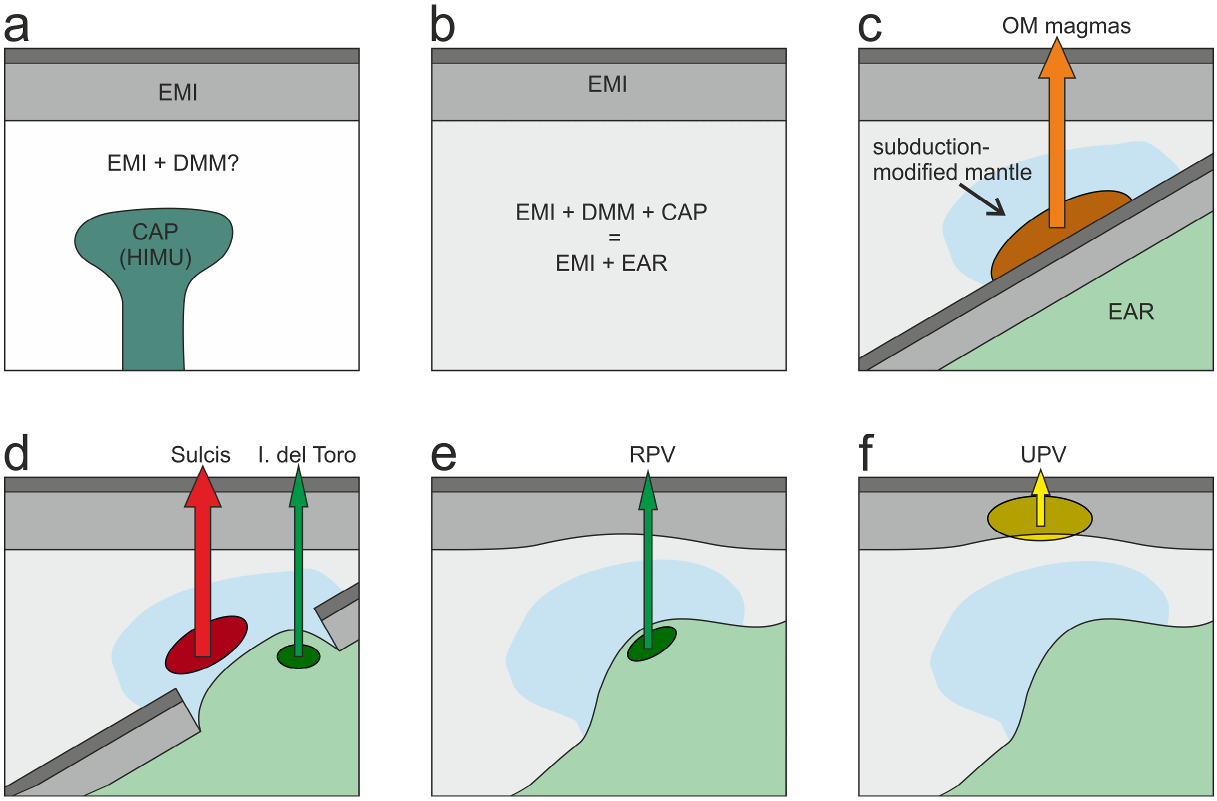

Fig. S7. Proposed geodynamic model of the mantle under Sardinia since the Cretaceous (not to scale). (**a**) In Cretaceous times the Central Atlantic Plume (CAP) started introducing a HIMU component into the mantle of the Euro-Mediterranean area, producing the prevalent EAR-like compositions by mixing with the pre-existing DMM mantle. In Sardinia, pre-existing asthenospheric mantle likely consisted of both EMI and DMM compositions, whereas the subcontinental lithospheric mantle presented dominant EMI component. (**b**) In Sardinia the CAP event produced an asthenospheric mantle with EMI+EAR compositions, whereas the lithospheric mantle was little affected, mostly retaining its EMI composition. (**c**) During the Oligo-Miocene, fluids released by the subducting slab favoured the flux melting of the mantle wedge and the production of calc-alkaline magmas. (**d**) At the end of the OM magmatic cycle, a slab tear opened a slab window below Sulcis, and cessation of fluids input resulted in the transition of magmatism from subduction-controlled to decompression-controlled as the mantle wedge continued to melt due to the existing extensional setting. Hot asthenospheric mantle with EAR composition ascended through the slab window, likely favouring further melting of the mantle wedge. Partial melts formed by decompression of this ascending mantle produced the Isola del Toro alkaline rocks at the very end of the OM magmatic cycle. (**e**) Extensional setting present since the late Miocene resulted in partial melting of the hotter, enriched, EAR mantle at the beginning of the Plio-Pleistocene magmatic cycle, producing the RPV in southern Sardinia. (**f**) As extension continued UPV magmas started to form below central and northern Sardinia in the subcontinental lithospheric mantle with dominant EMI compositions.